ELSEVIER

Journal of Power Sources 108 (2002) 128–138

JOURNAL OF POWER SOURCES

www.elsevier.com/locate/jpowsour

Ultra-thin passivating film induced by vinylene carbonate on highly oriented pyrolytic graphite negative electrode in lithium-ion cell

O. Matsuoka*, A. Hiwara, T. Omi, M. Toriida, T. Hayashi, C. Tanaka, Y. Saito, T. Ishida, H. Tan, S.S. Ono, S. Yamamoto

Materials Science Lab. R&D Center, Mitsui Chemicals Inc., 580-32 Nagaura, Sodegaura-City, Chiba 299-0265, Japan

Received 6 September 2001; accepted 19 December 2001

Abstract

We investigated the influence of vinylene carbonate, as an additive molecule, on the decomposition phenomena of electrolyte solution [ethylene carbonate (EC)—ethyl methyl carbonate (EMC) (1:2 by volume) containing 1 M $LiPF_6$] on a highly oriented pyrolytic graphite (HOPG) negative electrode by using cyclic voltammetry (CV) and atomic force microscopy (AFM). Vinylene carbonate deactivated reactive sites (e.g. radicals and oxides at the defects and the edge of carbon layer) on the cleaved surface of the HOPG negative electrode, and prevented further decomposition of the other solvents there. Further, vinylene carbonate induced an ultra-thin film (less than 1.0 nm in thickness) on the terrace of the basal plane of the HOPG negative electrode, and this film suppressed the decomposition of electrolyte solution on the terraces of the basal plane. We consider that this ultra-thin passivating film is composed of a reduction product of vinylene carbonate (VC), and might have a polymer structure. These induced effects might explain how VC improves the life performance of lithium-ion cells.

Keywords: Lithium-ion cell; HOPG; AFM; Vinylene carbonate; Additive molecule

1. Introduction

Decomposition of electrolyte solution on negatively polarized graphite anode has been known to deteriorate the performance of lithium-ion cells [1]. On the other hand, decomposition products form passivating film, which is impervious to solvent molecules but allows lithium ions to diffuse through its bulk. This passivating film is called solid electrolyte interface (SEI) [2,3]. Much studies on SEI, using various analytical techniques including FT-IR [4–6], X-ray photoelectron spectroscopy [7], scanning tunneling microscopy [8–10], and atomic force microscopy (AFM) [11–14], etc., have contributed to elucidation of the structure and formation mechanism of SEI [15,16]. The structure of a solvent molecule affects on the structure and formation mechanism of SEI. It is known that ethylene carbonate (EC) forms stable SEI on a graphite anode surface, whereas propylene carbonate (PC) does not [9,10]. Destruction of the carbon layer of graphite occurs in PC, and this destruction disables the charging of lithium-ion cells [9,10]. Demands for higher charging capacity, reliability and life performance have led to the development of novel solvent systems and additives that improve the performance of electrolyte solutions. Vinylene carbonate (VC) is an additive that improves the life performance of the lithium-ion cell [17]. VC allows the use of PC as the solvent of the electrolyte solution for lithium-ion cells that employ graphite as anodes [17]. Namely, VC must have some effect on the graphite anode, but the specific working mechanism remains unresolved. VC improves the performance of graphite negative electrode not only in PC based electrolyte solution, but also in EC based electrolyte solutions. EC is widely used as a solvent for electrolytes in commercially available lithium-ion cells. Clarification of the working mechanism of effective additives, such as VC, on reduction phenomena of electrolyte solutions on graphite negative electrode is vital to the development of a high performance electrolyte solution for lithium-ion cells. We have investigated the working mechanism of the VC additive in EC based electrolyte solution using AFM. The effects of VC on decomposition phenomena of solvents and on SEI formation in the EC based electrolyte solution on highly oriented pyrolytic graphite (HOPG) negative electrode surface are reported in this paper.

* Corresponding author. Tel.: +81-438-64-2317; fax: +81-438-64-2370.
E-mail address: osamu.matsuoka@mitsui-chem.co.jp (O. Matsuoka).

0378-7753/02/$ – see front matter
PII: S0378-7753(02)00012-5

2. Experimental

2.1. Materials

Cleaved HOPG surface (ZYH grade HOPG, Advanced Ceramics, Co.) was used as a model for graphite negative electrode. The HOPG negative electrode was prepared by cleaving with an adhesive tape in air, then dried in an argon-filled glove box with a dew point <−70 °C for 60 min. The pristine cleaved surface included terraces, step edges, and defects of the carbon layer. These sites act as reduction sites for electrolyte solutions. Step edges and defects act as reactive sites for lithium intercalation. The blank electrolyte solution was 1 M $LiPF_6$ dissolved in EC mixed with ethyl methyl carbonate (EMC) (1:2 by volume). VC, 2 wt.% was added to the blank electrolyte solution. The water content of each solution was less than 20 ppm.

2.2. Cyclic voltammetry and preparation of samples for AFM observation

Cyclic voltammetry (CV) were carried out with a three-electrode cell and a Solartron 1286 Electrochemical Interface (Schlumberger, Co.). Only the basal plane of the cleaved surface, of around 0.28 cm^2, was brought into contact with electrolyte solutions. Lithium wires were used as the reference and counter electrodes. The potential was scanned at 10 mV/s between 3.0 and 0.0 V, and the current response was recorded with a computer. All potentials were referred to as volts versus Li/Li^+. CV measurements were performed in the argon-filled glove box. For AFM sample preparation, the potential was scanned from 3.0 V to a given potential, and scanned back to 3.0 V at 10 mV/s. The cell was disassembled in the glove box, and then the HOPG electrode was transferred to a dry room with a dew point <−40 °C, where it was rinsed with pure EMC and dried in a vacuum evacuated by a rotary pump. By this rinsing, jelly-like substances [18] and precipitates that are soluble in EMC were removed from the electrode surface.

2.3. AFM observations

We employed an ex situ observation method after rinsing the electrode surface with EMC, for the following reasons: to determine whether there were components of SEI that were not stripped off easily in an electrolyte solution; to avoid the influence of the AFM tip during a potential sweep, which might result in scraping an SEI and disturbing a local field near the electrode surface; and to remove the over-layer comprised of jelly-like substances that might obscure the details of the electrode surface structure. AFM observation was carried out in air using the Tapping Mode™ of a NanoScope IIIa (Digital Instruments, Inc.) with a cantilever tip made of Si (L_0 = 125 μm, k_0 = 34 N/m, F_0 = 300 kHz, NCH-10T, NanoSensors). The free oscillation amplitude of the tip was in the range of 30–40 nm, and the reduced amplitude under observation was in the range of 20–30 nm. Extender electronics of NanoScope were used to allow the simultaneous collection of height and phase images. A contrast on a phase image is caused by a phase shift of the oscillation of the cantilever tip, and the phase shift is caused by a variation in surface properties such as elasticity, or in tip-sample interaction forces such as adhesion and viscoelasticity [19,20].

3. Results and discussion

3.1. CV measurements

Fig. 1a and b show cyclic voltammograms between 3.0 and 0.0 V for the pristine cleaved HOPG negative electrode surface in electrolyte solutions without and with VC, respectively. Reduction peaks in the potential range of 0.8–0.3 V are due to the decomposition of EC [8–14,21–23]. All

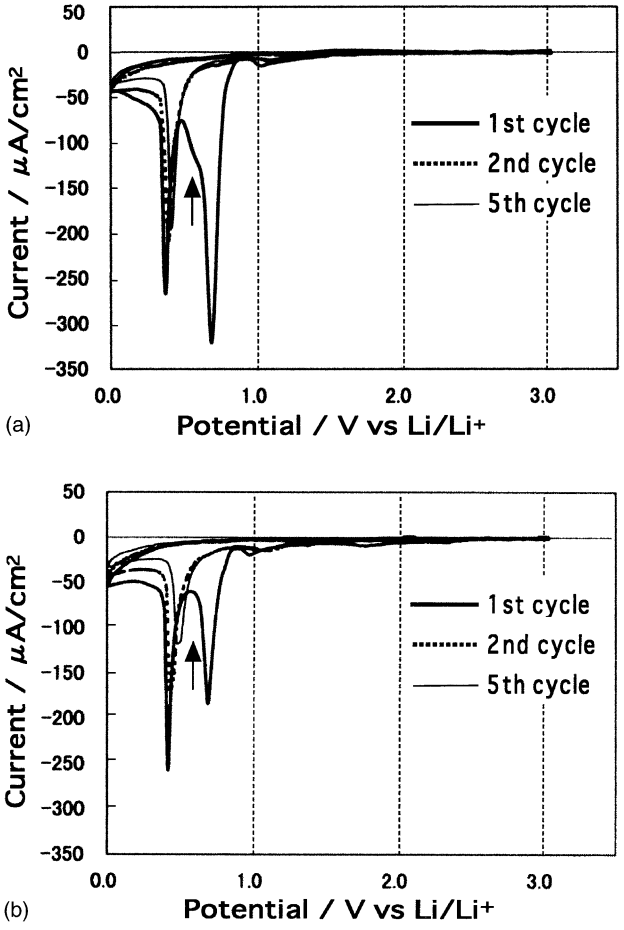

Fig. 1. Cyclic voltammograms of the HOPG negative electrode surface: (a) in the blank electrolyte solution (EC:EMC (1:1)/$LiPF_6$ (1 M)); (b) in the electrolyte solution containing VC (blank + VC (2 wt.%)). Sweep rate was 10 mV/s. Bold, dashed and fine lines correspond to the first, second, and fifth cycles, respectively. The reduction peak centered at 0.6 V is indicated by an arrow.

reduction peaks except the one centered at 0.4 V disappeared after the first cycle, and the intensity of the reduction peak centered at 0.4 V decreased in prolonged potential cycling. Thus, the reduction phenomenon corresponding to the reduction peak centered at 0.4 V was not completed in the first cycle at this potential sweep rate.

A remarkable difference on the cyclic voltammogram in the electrolyte solution containing VC compared with that in

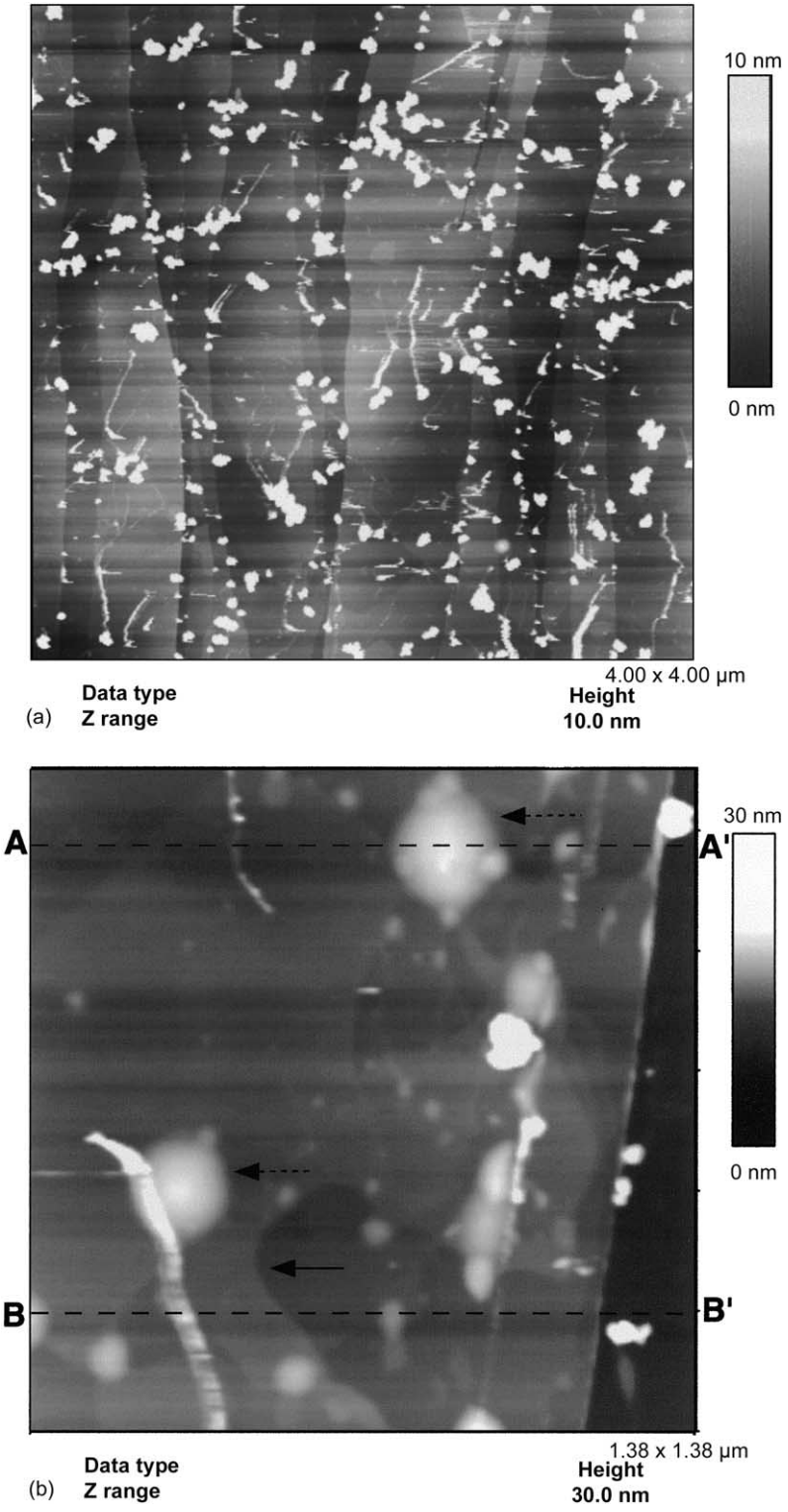

Fig. 2. Tapping Mode™ AFM images of the HOPG negative electrode surface in the blank electrolyte solution obtained at: (a) 1.0 V; (b, c) 0.7 V; (d) 0.45 V; (e) 0.1 V. Cross-sectional profiles in (b) are shown in (c). Bright particles might be the residues of lithium salt and solvents in image (a). Hill-like structure (fine arrow), blister (fine dashed arrow), swelling (bold arrow), and particle-shaped precipitates (bold dashed arrow) are indicated in AFM images.

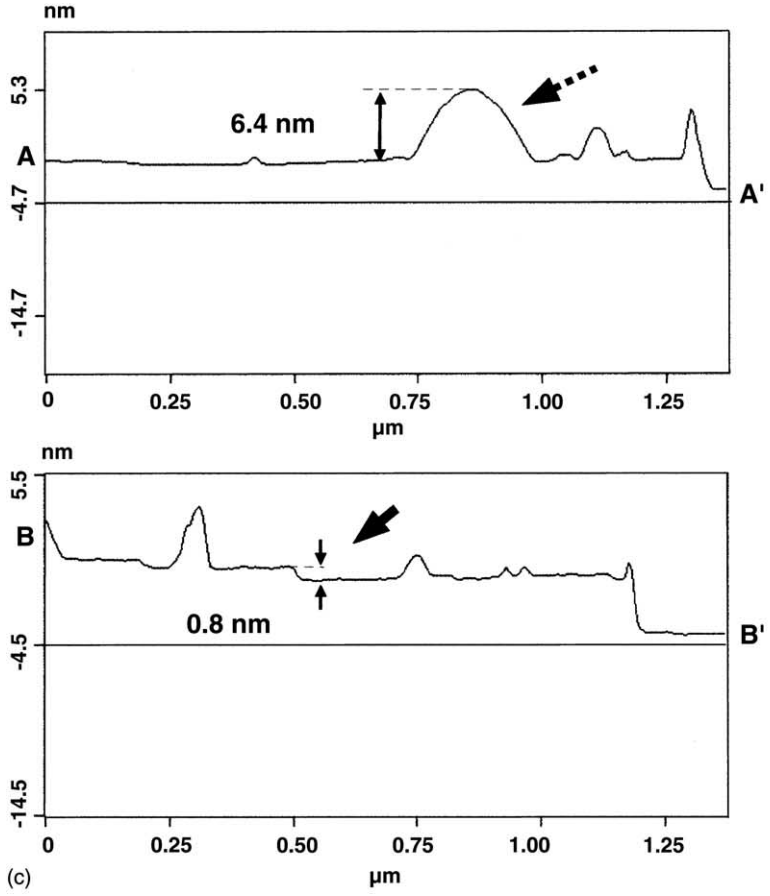

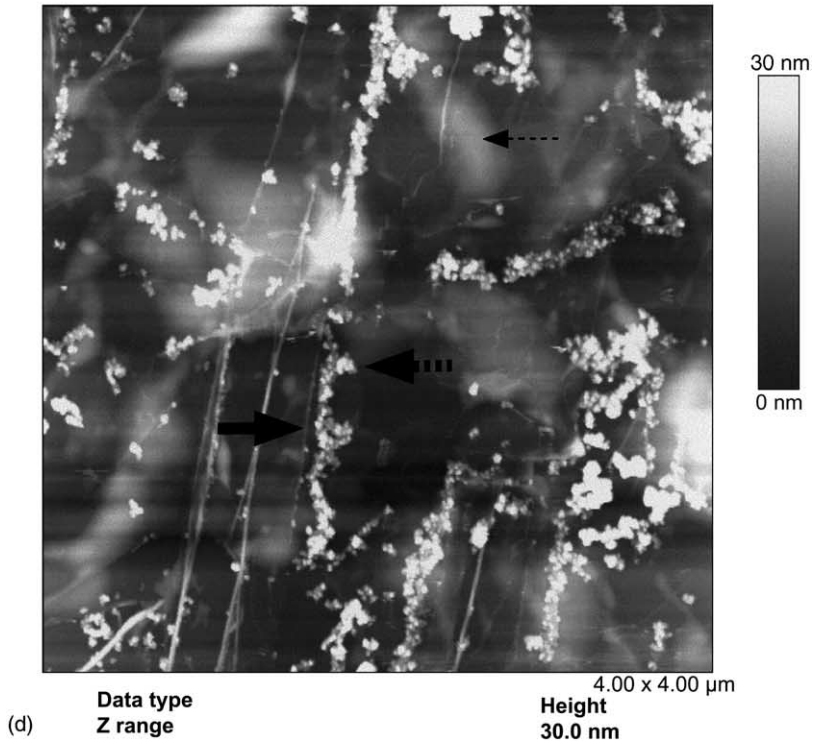

Fig. 2. (*Continued*).

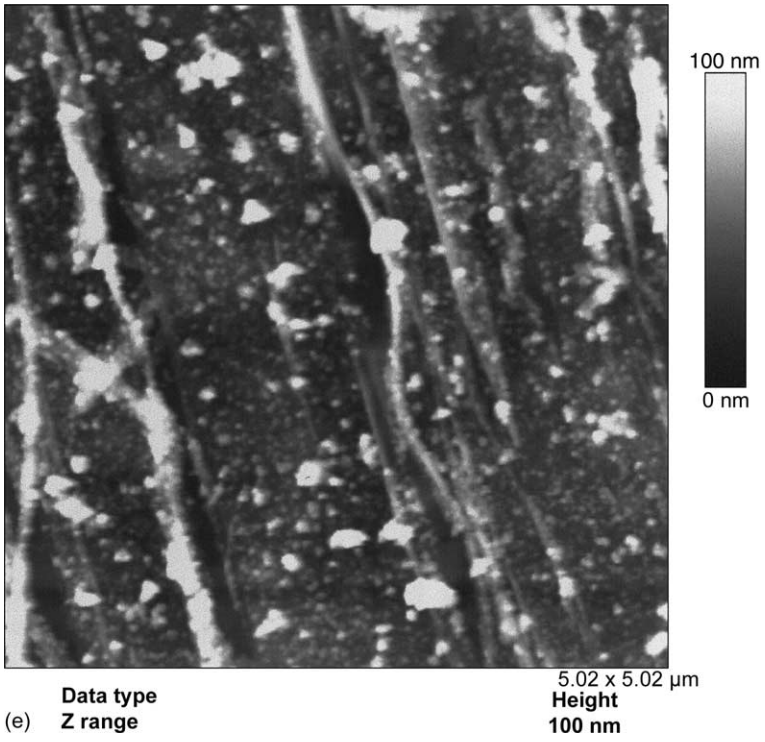

Fig. 2. (*Continued*).

the blank electrolyte solution was a diminution in the intensity of the reduction peak centered at 0.6 V (Fig. 1b). It has been reported in the literature that surface treatment using NF_3 plasma on carbon negative electrode reducing the reduction current at 0.6 V [24], and this might imply that the reactive sites were terminated by F atoms. Hence, VC might deactivate the reactive sites (e.g. radicals and oxides at the defects and the edge of carbon layer) on the HOPG negative electrode surface, and prevents further decomposition of the other solvents at the reactive site. We could not clearly assigned the reduction peak of VC, but small reduction current in the potential range of 2.0–1.5 V in the first cycle that was absent in the blank electrolyte solution could be due to the reduction of VC.

3.2. AFM observations

Fig. 2a–e show the morphology changes of the HOPG negative electrode surface at different potentials in the blank electrolyte solution. Particles considered as residues of lithium salt and solvents were recognized on the terrace of the basal plane of the HOPG negative electrode at 1.0 V, as shown in Fig. 2a. Flat hills in irregular shape, of about 0.80 nm in height and domes that were 2–10 nm in height were observed on the terrace of the basal plane at 0.7 V (Fig. 2b and c). These configurations have been known as the ''hill-like structures'' and the ''blisters'', respectively, and indicate the cointercalation of solvent [8–10,25]. Thus, the cathodic peak centered at 0.7 V is considered as representing the reduction of intercalated solvents. Swelling at step edges and particle-shaped precipitates appeared at 0.45 V (Fig. 2d). Hill-like structures were decreased, whereas blisters became notable and widened at 0.45 V. Particle-shaped precipitates must be decomposition products of the solvent, like those observed at 0.1 V. Swelling at step edges increased its volume and the terrace on the basal plane was covered with particle-shaped precipitates at 0.1 V, as shown in Fig. 2e. The tendency of the increase of particle-shaped precipitates on the terrace at lower potentials is similar to the results reported by Alliatta et al. [13] and Jeong et al. [14]. Therefore, these particle-shaped precipitates must be decomposition products of solvent such as lithium alkoxides, lithium alkyl carbonates and their compounds [4–6,13,14,26].

The reduction peak centered at 0.4 V was considered to be correlated with the growth of the swelling at step edges. The step edge is the site for lithium intercalation, hence the decomposition causing swelling at the step edge might be accompanied by the initial stage of the lithium-ion intercalation process. Fig. 3a and b show a magnified topographic image and the corresponding phase image, respectively, of the swelling at the edge at 0.1 V. A change in contrast on a phase image is caused by a variation in surface properties such as elasticity, or in tip-sample interaction forces such as adhesion and viscoelasticity [19,20]. Therefore, a homogeneous material does not give any contrast changes on phase image. The height difference of terraces shows no contrast in the phase image (Fig. 3a and b). The phase contrast in the region labeled A of the swelling at the step edge was different from that in the region labeled B, as shown in Fig. 3b. The contrast in the region A was comparable to that

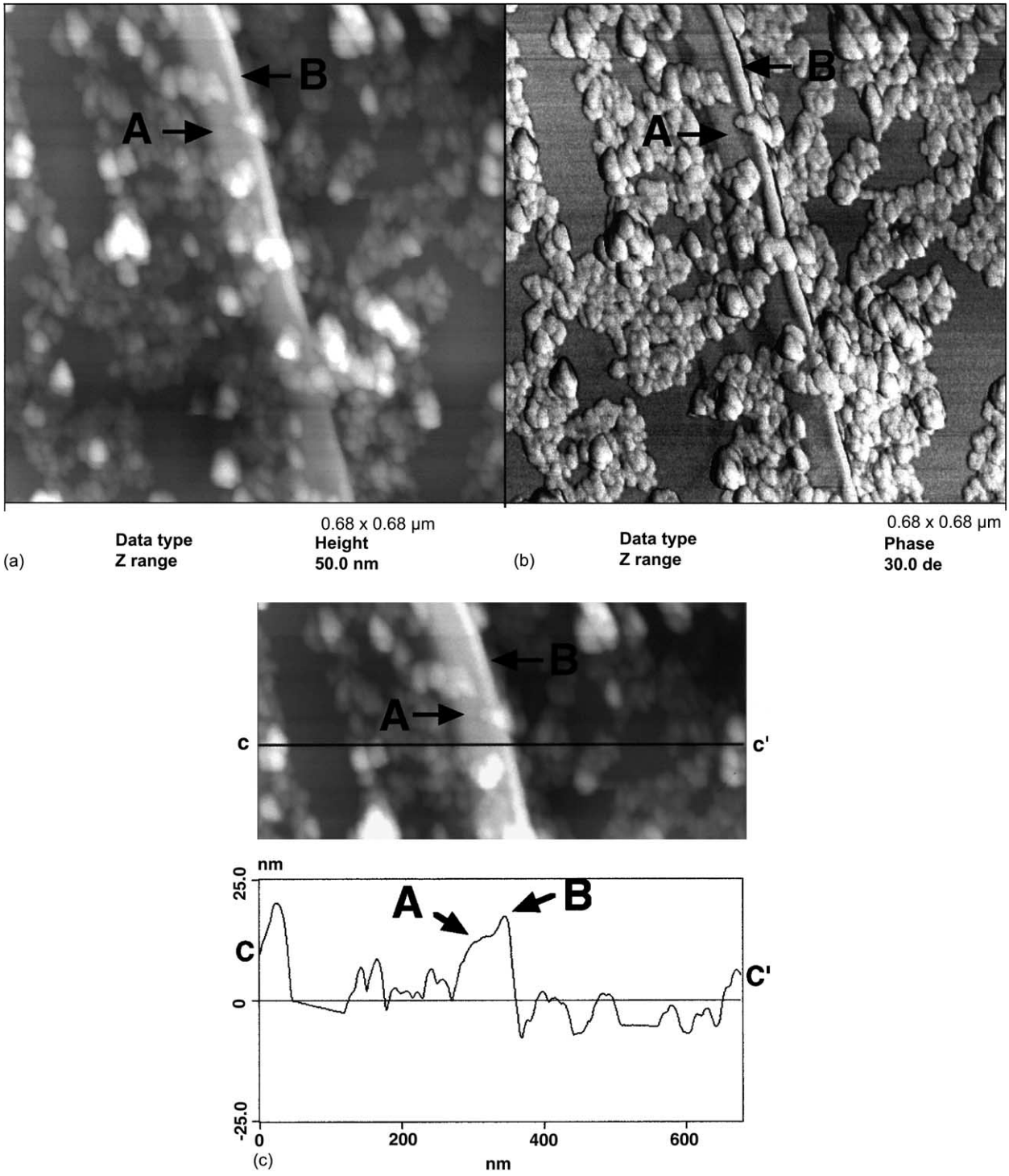

Fig. 3. Tapping Mode™ AFM images on the swelling at the step edge in the blank electrolyte solution: (a) topographic image; (b) phase image; (c) cross-sectional profile of the swelling at the step edge.

of a terrace of the basal plane, whereas the contrast in the region B was similar to that of the precipitates on a terrace of the basal plane. These contrast changes indicate that swelling in the region A exists in the interlayer space, and that in the region B has been pushed out of the interlayer space. These results imply that the decomposition of electrolyte solution at step edges occurs in an interlayer space neighboring a step edge. The substance comprising the swelling at step edges is considered to be the SEI that plays an important role for lithium-ion intercalation and de-intercalation. The component of this substance could be different from the particle-shaped precipitates on the terrace, because the component of SEI at the edge plane has been reported to differ from that on the basal plane [26].

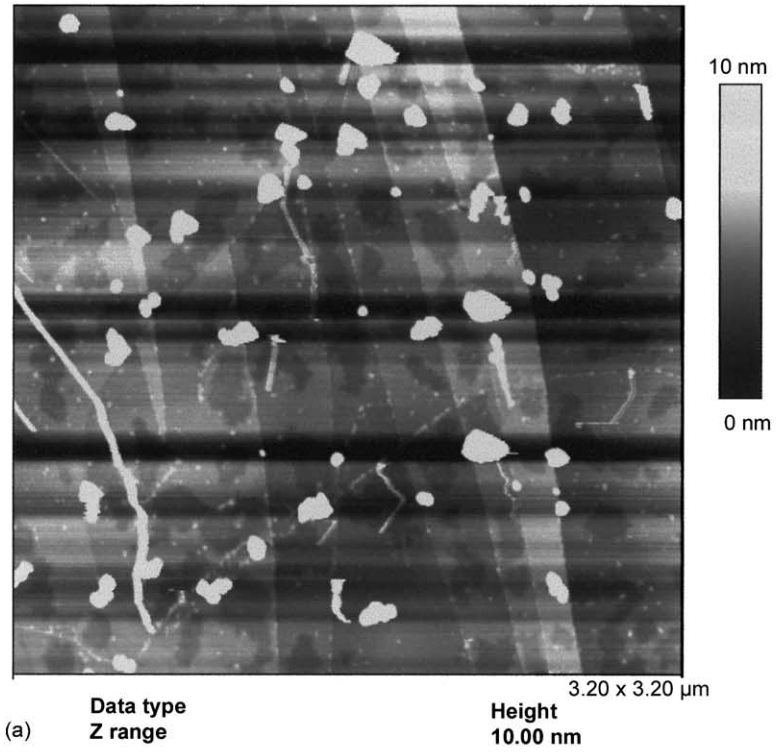

Fig. 4. Tapping Mode™ AFM images of the HOPG negative electrode surface in the electrolyte solution containing VC at: (a, b) 1.0 V; (c) 0.7 V; (d) 0.45 V; (e) 0.1 V. A cross-sectional profile in (a) is shown in (b). Hill-like structure (fine arrow), blister (fine dashed arrow), swelling (bold arrow), and particle-shaped precipitates (bold dashed arrow) are indicated in AFM images.

Fig. 4a–e show AFM images on the HOPG negative electrode surface in the electrolyte solution containing VC at different potentials. A patch-shaped configuration on the terrace of the basal plane that was made from height difference appeared at 1.0 V in the electrolyte solution containing VC (Fig. 4a and b). This configuration on the terrace shows a phase contrast, as shown in Fig. 5a and b, and was not recognized in the blank electrolyte solution. In this measuring condition for phase imaging, the height difference of a terrace on the basal plane resulted in no phase contrast, as can be seen in these images. Two possible explanations for this configuration might be considered:

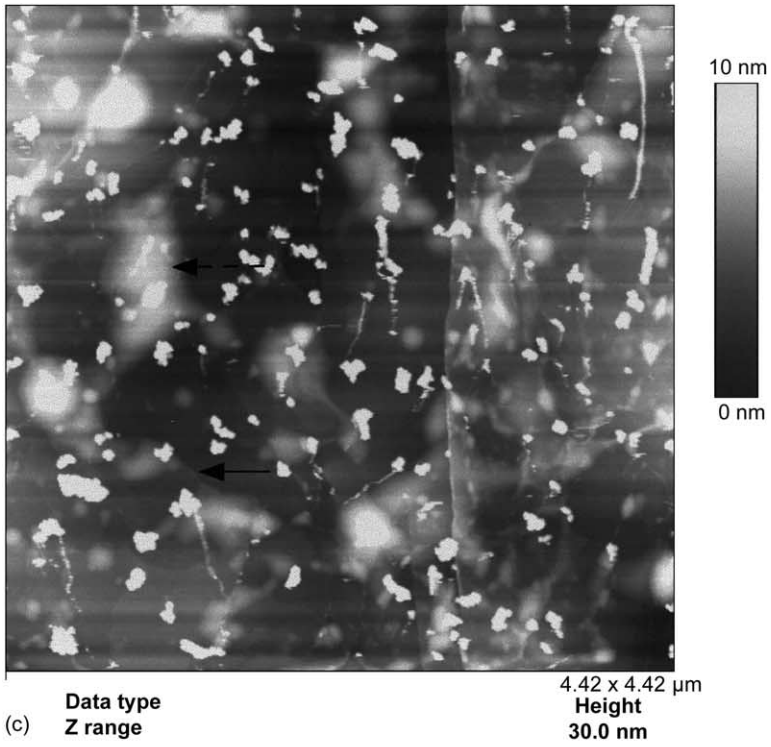

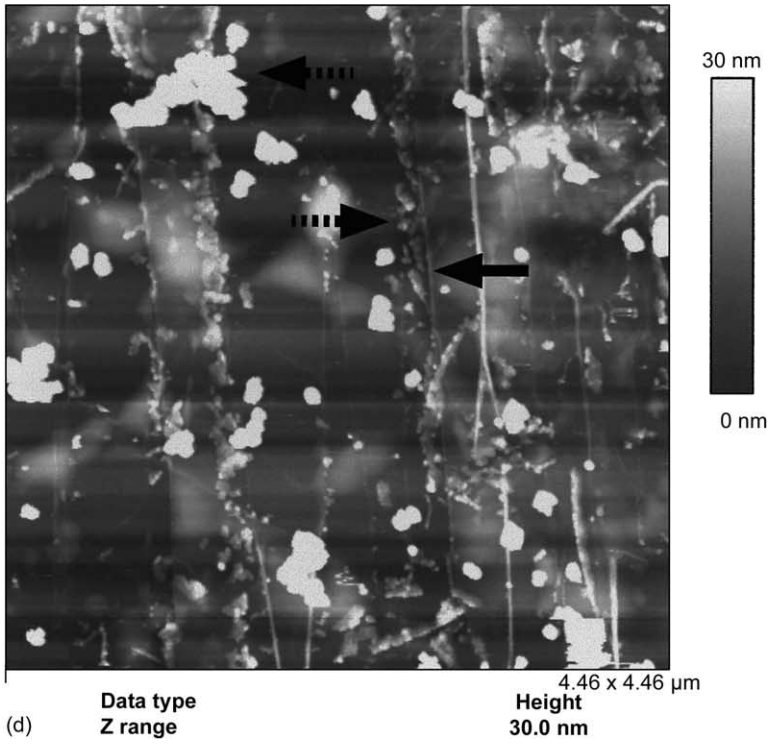

Fig. 4. (*Continued*).

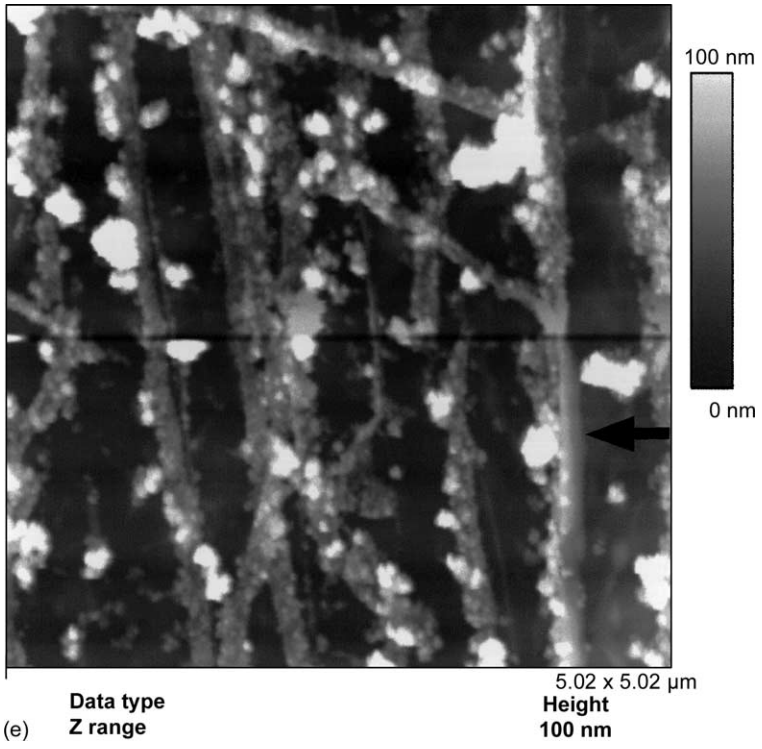

Fig. 4. (*Continued*).

(1) an over-layer formed on the basal plane; (2) a hill-like structure originated from cointercalation. The latter must be ruled out because hill-like structures and blisters give no phase contrast in this measuring condition, as shown in Fig. 6a and b. Therefore, the configuration observed at 1.0 V is considered to be an over-layer formed on the terrace of the basal plane. The thickness of this over-layer is about 0.7 nm, as shown in Fig. 4b. Many defects, recognized as holes, on

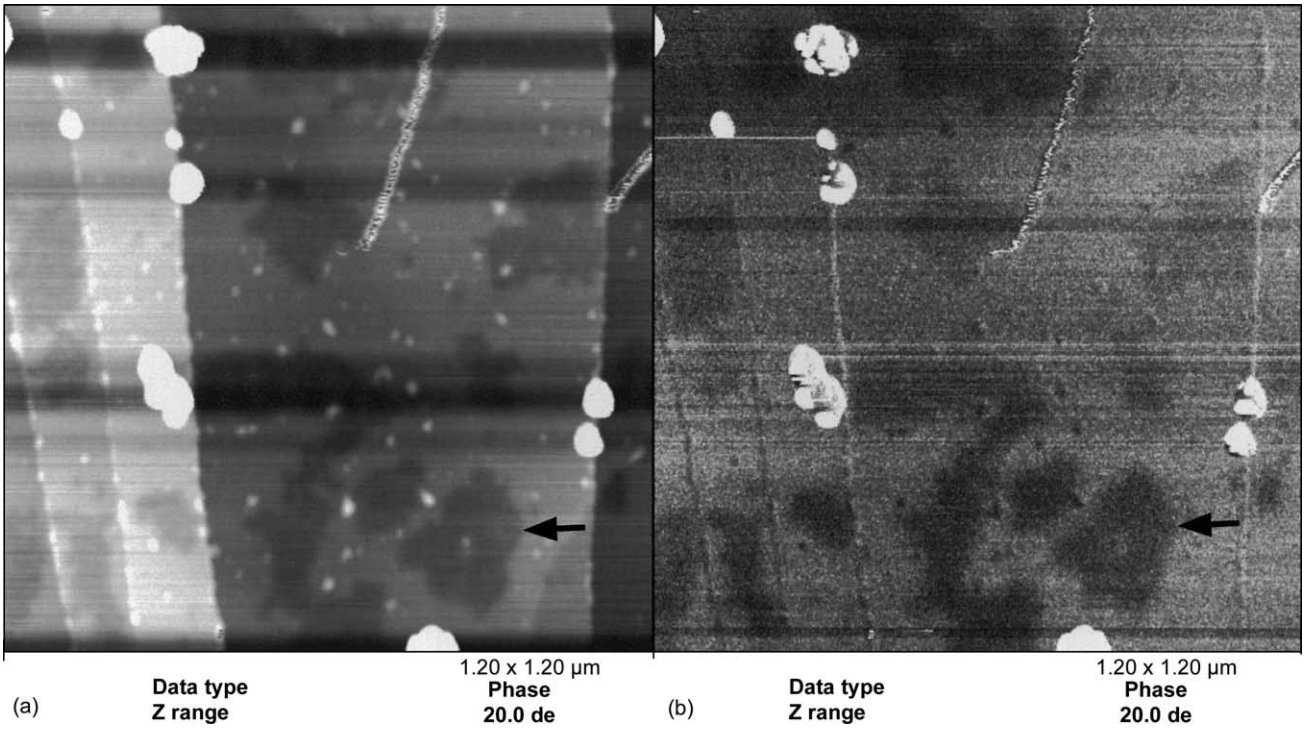

Fig. 5. Tapping Mode™ AFM images of the over-layer at 1.0 V in the electrolyte solution containing VC: (a) topographic image; (b) phase image. Defects of the over-layer are indicated by arrows.

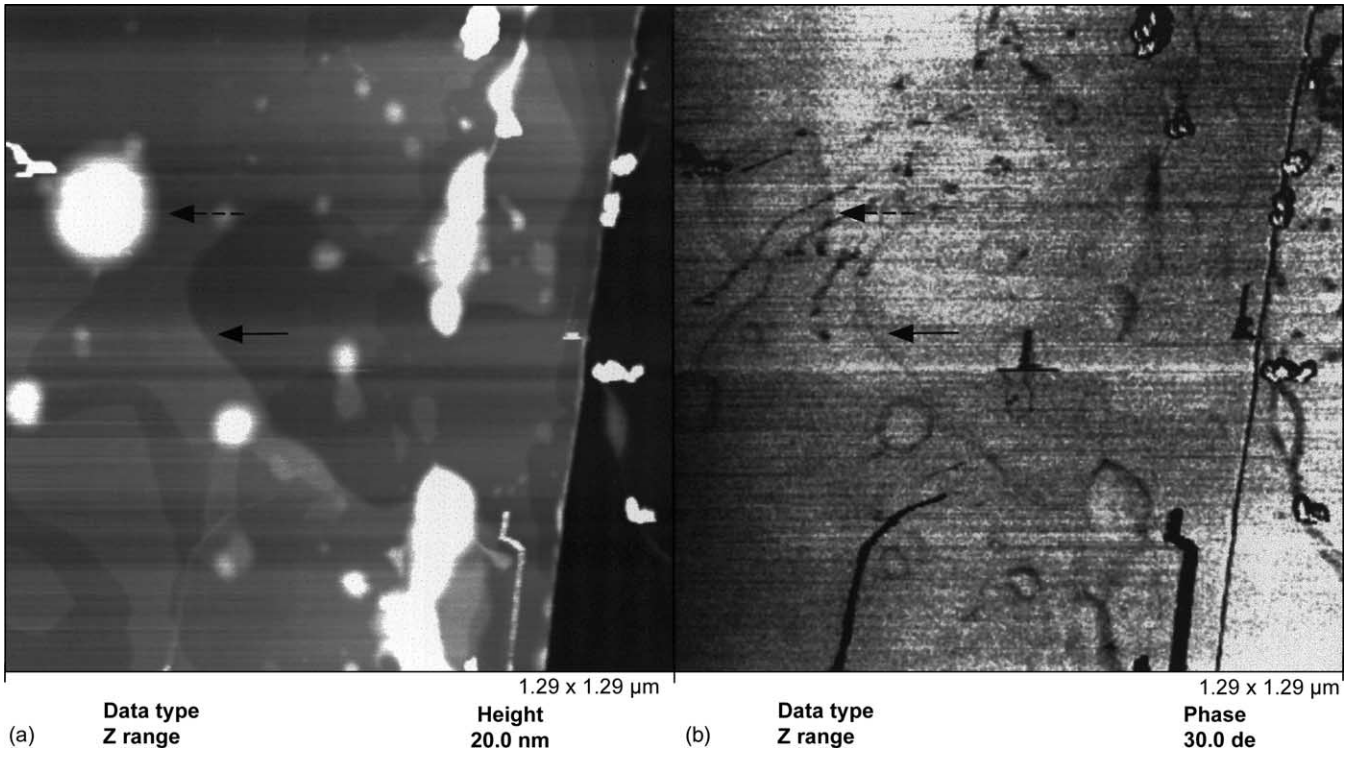

Fig. 6. Tapping Mode™ AFM images of the hill-like structure and blister at 0.8 V in the blank electrolyte solution: (a) topographic image; (b) phase image. The hill-like structure (fine arrow) and the blister (fine dashed arrow) are indicated in AFM images.

this thin over-layer indicate that the potential sweep rate in this experiment must be too first to create a complete over-layer formation in the first cycle. We consider that this over-layer is composed of a reduction product of VC, and might have a polymer structure.

Another noticeable feature is a smaller amount of precipitates on the basal plane at 0.1 V in the electrolyte solution containing VC than in the blank electrolyte solution, as shown in Fig. 4e. It is reasonable to consider that the over-layer observed at 1.0 V suppresses the solvent reduction on the terrace of the basal plane of the HOPG negative electrode surface. Namely, the presence of VC induced a thin passivating film on the terrace of the basal plane.

The morphologies of the HOPG negative electrode surface at 0.7 and 0.45 V were similar to those in blank solution, as shown in Fig. 4c and d, respectively. Hill-like structures and blisters were observed at 0.7 V, and swelling at the step edge was observed at 0.45 V. These results indicate that the cointercalation and the formation of the substance comprising the swelling at step edges were not completely inhibited by the presence of VC. The morphology corresponding to the reduction peak centered at 0.6 V could not be clearly distinguished in this observation.

4. Conclusions

The influence of vinylene carbonate as an additive on the decomposition phenomena of electrolyte solution (1 M $LiPF_6$/EC + EMC system) on the HOPG negative electrode surface was studied by using CV and AFM. Vinylene carbonate deactivated reactive sites (e.g. radicals and oxides at the defects and the edge of carbon layer) on the cleaved surface of the HOPG negative electrode, and prevented further decomposition of the other solvents there. Further, vinylene carbonate induced an ultra-thin film (less than 1.0 nm in thickness) on the terrace of the basal plane of the HOPG negative electrode, and this film suppressed the decomposition of electrolyte solution on the terraces of the basal plane. We consider that this ultra-thin passivating film is composed by a reduction product of VC, and might have a polymer structure. These induced effects might explain how VC improves the life performance of lithium-ion cells.

Acknowledgements

The authors are grateful to Prof. Z. Ogumi and Associate Prof. M. Inaba of Kyoto University for useful discussion.

References

[1] M. Winter, P. Navok, A. Monnier, J. Electrochem. Soc. 145 (1998) 428.
[2] E. Peled, J. Electrochem. Soc. 126 (1979) 2047.
[3] E. Peled, in: J.P. Gabano (Ed.), Lithium Batteries, Academic Press, New York, 1983, p. 43.

[4] Y. Ein-Eli, S.R. Thomas, V. Kock, B. Markovsky, A. Zaban, S. Luski, Y. Carmeli, H. Yamin, J. Electrochem. Soc. 144 (1997) 1159.
[5] D. Aubach, B. Markovsky, I. Weissman, E. Levi, Y. Ein-Eli, Electrochim. Acta 45 (1999) 67.
[6] Y.-G. Ryu, S.-I. Pyun, J. Electroanal. Chem. 433 (1997) 97.
[7] D. Bar-Tow, E. Peled, L. Burstein, J. Electrochem. Soc. 146 (1999) 824.
[8] M. Inaba, Z. Siroma, A. Funabiki, Z. Ogumi, T. Abe, Y. Mizutani, M. Asano, Langmuir 12 (1996) 1535.
[9] M. Inaba, Z. Siroma, Y. Kawatake, A. Funabiki, Z. Ogumi, J. Power Sources 68 (1997) 221.
[10] Z. Ogumi, M. Inaba, Bull. Chem. Soc. Jpn. 71 (1998) 521.
[11] K.A. Hirasawa, T. Sato, H. Asahina, S. Yamaguchi, S. Mori, J. Electrochem. Soc. 144 (1997) L81.
[12] A.C. Chu, J.Y. Josefowick, G.C. Farhington, J. Electrochem. Soc. 144 (1997) 4161.
[13] D. Alliatta, R. Kota, P. Novak, H. Siegenthaler, Electrochem. Commun. 2 (2000) 436.
[14] S.-K. Jeong, M. Inaba, T. Abe, Z. Ogumi, J. Electrochem. Soc. 148 (2001) A989.
[15] R. Yazami, Electrochim. Acta 45 (1999) 87.
[16] D. Aurbach, J. Power sources 89 (2000) 206.
[17] B. Philippe, B. Jean-Marie, P. Francoise, B. Michel, J. Cristophe, B. Sylvie, H. Sylvie, S. Bernard, in: Proceedings of the 10th International Meeting on lithium Batteries, Abstracts, No. 286.
[18] K. Tatsumi, K. Zaghib, S. Koike, T. Sakai, H. Shioyama, in: Proceedings of the of the 39th Battery Symposium in Japan on Extended Abstracts, Sendai, 1998, pp. 449–450.
[19] D.A. Chernoff, Proc. Microsc. Microanal. (1995) 888.
[20] D.A. Chernoff, Nanonations Winter 1996, Digital Instruments, Santa Barbara, CA., 1996, p. 6.
[21] Z.X. Shu, R.S. McMillan, J.J. Murray, J. Electrochem. Soc. 140 (1993) 922.
[22] P. Novak, F. Joho, J.-C. Panitz, O. Haas, J. Power Sources 81 (1999) 212.
[23] R. Imhof, P. Novak, J. Electrochem. Soc. 145 (1998) 1081.
[24] T. Fukutsuka, T. Abe, M. Inaba, Z. Ogumi, A. Tasaka, in: Proceedings of the 41st Battery Symposium in Japan on Extended Abstracts, Nagoya, Japan, 2000, pp. 592–593.
[25] J.O. Besenhard, M. Winter, J. Yang, W. Biberacher, J. Power Sources 54 (1995) 228.
[26] E. Peled, D. Bar-Tow, A. Merson, A. Gladkich, L. Burstein, D. Golodnitsky, J. Power Sources 97–98 (2001) 52.